Lane-free Traffic with Connected and Automated Vehicles - An Optimal Control Approach

V. K. Yanumula*, P. Typaldos, D. Troullinos, M. Malekzadeh, I. Papamichail, and M. Papageorgiou

Dynamic Systems and Simulation Laboratory, Technical University of Crete, Chania, Greece
{karteek, ptypaldos, dtroullinos, mmalek, ipapa, markos}@dssl.tuc.gr
* Corresponding author

Extended Abstract submitted for presentation at the 11th Triennial Symposium on Transportation Analysis conference (TRISTAN XI)
June 19-25, 2022, Mauritius Island

March 26, 2022

Keywords: Lane-free traffic, connected and automated vehicles, optimal path planning, model predictive control

1 INTRODUCTION

Inefficient usage of the road space is a major reason for traffic congestion, which entails increased delays and fuel consumption and increased emissions. In addition, the vast majority of road accidents are caused due to erratic human driving. Despite extensive research on traffic management, congestion and accidents occur excessively across the world. To mitigate these issues, connected and automated vehicles (CAVs) seem promising (Montanaro *et al.*, 2019). When the roads are largely populated with CAVs, using Vehicle-to-Vehicle (V2V) and Vehicle-to-Infrastructure (V2I) information sharing, lanes may become unnecessary, as they waste lateral road space due to variations in the width of vehicles, and necessitate accident-prone lane-changing manoeuvres. With the lane-free traffic paradigm proposed by (Papageorgiou *et al.*, 2021), the lane structure of traffic, designed to facilitate human driving, can be dropped in the era of CAVs in favour of increased safety and efficiency. In fact, the real-time perception capabilities of automated vehicles are superb, compared to human drivers, due to a large number of sensors with 360° scanning and multiple scans per second. The CAVs, backed with appropriate path planning algorithms, may move on a lane-free road, whereby vehicle movement may be influenced not only by other vehicles in front of them (as with human driving), but also by vehicles behind, something that is referred to as 'nudging' (Karafyllis *et al.*, 2020). The current work presents an optimal control problem (OCP) approach for path planning, without the need for discrete lateral positioning thanks to lane-free driving that renders lane changing obsolete. The dynamic driving environment calls for frequent path planning updates over short time horizons (e.g. 8 s), as long horizons inevitably entail outdated predictions on surrounding traffic. An efficient feasible direction algorithm (FDA) (Papageorgiou *et al.*, 2016) is used to solve (in 15.9 ms on average) the OCP for each vehicle in a model predictive control (MPC) frame, which enables the CAVs to use updated information.

2 OPTIMAL CONTROL PROBLEM (OCP)

Due to computer-based decision making in real time, the OCP consists of a discrete-time kinematic system model, with bounded control input, and an objective function, whose minimization

reflects a number of goals. More specifically, each ego vehicle (EV) is described by the following set of equations, with real-valued positioning on both longitudinal and lateral directions, thanks to the lane-free structure.

$$x_1(k+1) = x_1(k) + Tx_3(k) + \frac{1}{2}T^2u_1(k) \tag{1a}$$
$$x_2(k+1) = x_2(k) + Tx_4(k) + \frac{1}{2}T^2u_2(k) \tag{1b}$$
$$x_3(k+1) = x_3(k) + Tu_1(k) \tag{1c}$$
$$x_4(k+1) = x_4(k) + Tu_2(k) \tag{1d}$$

where T is the time step; k is the integer time index, related to continuous time t via $t = kT$; the states x_1, x_2 are longitudinal and lateral positions of the vehicle centre, respectively; x_3, x_4 are longitudinal and lateral speeds, respectively; while u_1 and u_2 are longitudinal and lateral accelerations, respectively, i.e. the control inputs. The CAVs are essentially moving longitudinally, along a highway or arterial, with lateral road boundaries; consequently, the decoupled model (1) is sufficiently accurate, particularly under the influence of an appropriate term in the objective function that discourages infeasible lateral steering. The upper and lower bounds on the accelerations are as follows

$$u_{\min 1}(x_3) \leq u_1(k) \leq u_{\max 1} \tag{2a}$$
$$u_{\min 2}(x_2, x_4) \leq u_2(k) \leq u_{\max 2}(x_2, x_4) \tag{2b}$$

As seen, the longitudinal upper bound is constant, reflecting vehicle capabilities and passenger convenience. The longitudinal lower bound and lateral bounds are state-dependent. Specifically, the longitudinal lower bound is designed to prevent the vehicle from reaching negative speeds at the next time step, i.e. to ensure $x_3(k+1) \geq 0$; from which, using state equation (1c), we obtain $u_1(k) \geq -\frac{1}{T}x_3(k)$. In addition, the lower bound needs to consider a comfortable limit UMIN_1 for smooth ride quality; hence, the longitudinal lower bound is defined as

$$u_{\min 1} = \max\left\{-\frac{1}{T}x_3(k), \text{UMIN}_1\right\} \tag{3}$$

Vehicles are considered to be moving on unfolded roads that have straight lines as road boundaries. The CAVs should drive at times k and $k+1$ so as to stay inside the road boundaries at $k+2$, i.e., $e_w \leq x_2(k+2) \leq r_w - e_w$, where r_w is the road width and e_w is the half width of EV. If EV is moving on the road boundary, it should satisfy $x_4(k+2) = 0$ to stay at least on the road boundary. Thus, using again the state equations (1b) and (1d), the state-dependent bounds on lateral acceleration are as follows

$$-\frac{1}{T^2}[x_2(k) - e_w] - \frac{3}{2T}x_4(k) \leq u_2(k) \leq -\frac{1}{T^2}\left[x_2(k) - r_w + e_w\right] - \frac{3}{2T}x_4(k) \tag{4}$$

The bounds in (4) represent a dead-beat controller with high magnitudes. Considering passenger comfort and vehicle capabilities, the controller gains are chosen more moderate, and the generalized representation is given as

$$u_{\min 2}(x_2(k), x_4(k)) = -K_{\text{lat1}}[x_2(k) - e_w] - K_{\text{lat2}}x_4(k) \tag{5a}$$
$$u_{\max 2}(x_2(k), x_4(k)) = -K_{\text{lat1}}[x_2(k) - r_w + e_w] - K_{\text{lat2}}x_4(k) \tag{5b}$$

with $0 < K_{\text{lat1}} \leq 1/T^2$ and $0 < K_{\text{lat2}} \leq 3/(2T)$ as feedback controller gains chosen appropriately to prevent road departures, as EV may reach the road boundaries asymptotically.

The objective function is made up of several sub-objectives to account for passenger comfort, fuel consumption, target speed, collision avoidance and infeasible steering, as follows:

$$J=\sum_{k=0}^{K-1}\left\{w_1(u_1(k))^2+w_2(u_2(k))^2+w_3[x_3(k)-v_{d_1}]^2+w_4[x_4(k)-v_{d_2}]^2+w_5\sum_{i=1}^{n}[c_i(\boldsymbol{x},\boldsymbol{o}_i)]+w_6 f_c\right\} \quad (6)$$

The first two terms aim for passenger comfort and also for minimization of fuel consumption. The third and fourth terms help the EV to reach its target speeds, v_{d_1} and v_{d_2} in longitudinal and lateral directions, respectively. An *interaction zone* with equal length on upstream and downstream directions is defined to communicate with other vehicles that are treated as obstacles (OVs). The length of the interaction zone equals to the product of the longitudinal desired speed and the planning horizon K. For n OVs with relative position of their centers (o_{i1}, o_{i2}) inside the interaction zone and with speeds (o_{i3}, o_{i4}), the obstacle avoidance sub-objective is defined as $w_5 \sum_{i=1}^{n}[c_i(\boldsymbol{x}, \boldsymbol{o}_i)]$, where, for i^{th} OV, we use an ellipsoid-like function,

$$c_i(\boldsymbol{x},\ \boldsymbol{o}_i) = 1 - \tanh\left[\left(\frac{x_1-\delta_{o_1}}{r_1}\right)^{p_1}+\left(\frac{x_2-o_{i2}}{r_2}\right)^{p_2}\right]+\frac{1}{\left[\left(\frac{x_1-\delta_{o_1}}{r_3}\right)^{p_3}+\left(\frac{x_2-o_{i2}}{r_4}\right)^{p_4}\right]^{p_5}+1} \quad (7)$$

with exponents p_1 to p_5 influencing the ellipsoid shape. The ellipsoid function (7) is rather complex, as it needs to adequately address two requirements. Firstly, its iso-cost curves around the vehicle should approximate and fully cover the rectangular vehicle shape, without wasting too much space around the rectangle; this is achieved by the first term in (7) with appropriate values for the exponents p_1 and p_2. However, that term by itself exhibits a very flat shape at the interior of the rectangle, which implies accordingly low gradient values and therefore slow convergence of the numerical solution algorithm for the optimal control problem. Therefore, the second term is added, which does not alter the iso-cost curves around the vehicle, but provides a steep increase of the overall function (hence strong gradient values) at the interior of the vehicle-rectangle. Moreover,

$$r_1 = 0.5\,(L_i + \omega_{x_1} x_3 + \omega_{x_1} o_{i3}) \quad (8a)$$

$$r_2 = 0.5\left(W_i + \omega_{x_2}\left[\tanh(o_{i2}-x_2)\,(x_4-o_{i4}) + \sqrt{[\tanh(o_{i2}-x_2)\,(x_4-o_{i4})]^2+\epsilon_w}\right]\right) \quad (8b)$$

where, $L_i = l_e + l_{oi}$ with l_e and l_{oi} being 1.3 times the lengths of EV and OV; $W_i = w_e + w_{oi}$ with w_e and w_{oi} being 1.2 times the widths of EV and OV; ω_{x_1} and ω_{x_2} are time-gap like parameters. The ellipsoid is positioned longitudinally at $\delta_{o_1} = o_{i1} - \omega_{x_1}\,(x_3 - o_{i3})\,/2$; $r_3 = 0.5 r_1$ and $r_4 = 0.5 r_2$. To visualize, consider EV positioned at (10, 4) m and an OV at (30, 5.1) m, with length of each equal to 5 m, width equal to 1.8 m; longitudinal speed of EV at 35 m/s and of OV at 30 m/s. The contour plot of (7) with $p_1 = 6$, $p_2 = p_3 = p_4 = p_5 = 2$, $\omega_{x_1} = 0.35$, $\omega_{x_2} = 0.5$ is shown in Figure 1, in which, the red box represents the physical dimensions (L_i, W_i), while, the green box represents ellipsoid dimensions. It may be seen that the ellipsoid may cause both repulsing and nudging influence to other vehicles.

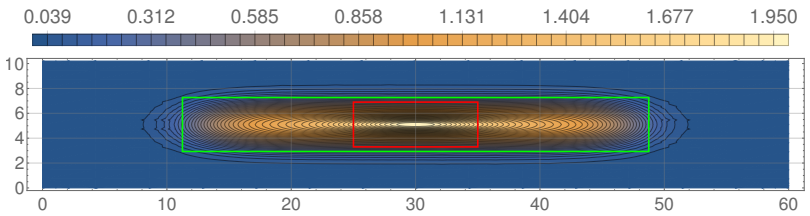

Figure 1 – *Sample of OV ellipsoid.*

In order to discourage the vehicle from taking infeasible values of steering, the following sub-objective that increases quadratically if the lateral speed exceeds β times the longitudinal speed, for some small $\beta > 0$ is considered,

$$f_c = \begin{cases} (\beta x_3(k) - x_4(k))^2 & \text{if } x_4(k) > \beta x_3(k) \\ (\beta x_3(k) + x_4(k))^2 & \text{if } x_4(k) < -\beta x_3(k) \\ 0 & \text{otherwise} \end{cases} \tag{9}$$

The sub-objective function for obstacle avoidance may not fully guarantee collision-free movement, which calls for additional measures in the rare case that the generated trajectory includes a collision. Thus, each OCP trajectory generation is checked for possible collisions. If that is detected, the OCP is resolved with stricter bounds on the control input. In case of longitudinal collision, the ego vehicle uses the rear bumper position of that OV (plus a time gap) as a moving boundary. Then, the state-dependent lower and upper bounds of the longitudinal acceleration are re-defined, similarly to lateral bounds, as,

$$u_{\text{min1}} = \max\left\{-\frac{1}{T}x_3(k), \text{UMIN}_{11}\right\} \tag{10a}$$

$$u_{\text{max1}} = \max\left\{u_{\text{min1}}, K_{\text{long}_1}(-x_1(k) + x_{1\text{Lim}}) + K_{\text{long}_2}(o_{i3}(k) - x_3(k)) + u_{1o}(k)\right\} \tag{10b}$$

where, $x_{1\text{Lim}} = \left(o_{i1}(k) - \frac{l_e}{2} - \frac{l_{oi}}{2} - \omega_{x_1\text{emer}}x_3(0)\right)$ and UMIN_{11} is an emergency value to allow the EV to decelerate harder. On the other hand, in case of a lateral collision, the movement of EV is restricted laterally by assuming virtual road boundaries that form a narrow corridor around the current lateral position of the EV, while the bounds on lateral acceleration remain unchanged.

3 RESULTS AND CONCLUSION

Extended simulations were performed using the TrafficFluid-Sim (Troullinos *et al.*, 2021), an extension designed for lane-free traffic to be used with the SUMO (Simulation of Urban MObility) simulator (Lopez *et al.*, 2018). All the vehicles are assumed to be moving on an unfolded ring-road of 1.0 km length and 10.2 m width, with eight different vehicle sizes, and target speeds randomly assigned between 25 and 35 m/s. The flows achieved during the last ten minutes of 1-hour simulations for different densities are given in Table 1. On a road width that is equivalent to three conventional lanes, high flow values are reached on the account of lane-free environment.

Table 1 – *Flow outcomes for given densities.*

Density (veh/km)	50	100	150	200	250	300	350	400	450	500
Flow (veh/hr)	5354	10464	14899	18381	15813	13003	10615	8156	5707	2878

Videos reflecting vehicle driving on the ring-road may be viewed at `https://bit.ly/TF-OPP`. The optimal path planning for CAVs seems promising and delivers good results. Multiple OCPs are solved at each time in an MPC framework with event-based updating to generate finite horizon trajectories for respective EVs. The proposed method results in high flows, small computation times and smooth trajectories for passenger comfort. More results are omitted due to lack of space and will be included in the presentation and full paper. Related work is going on to consider ramps, variable road widths and complex networks.

Acknowledgement

This research received funding from the European Research Council under the EU Horizon 2020 Programme / ERC Grant no. 833915, project TrafficFluid, see: `https://www.trafficfluid.tuc.gr`

References

Karafyllis, Iasson, Theodosis, Dionysios, & Papageorgiou, Markos. 2020. Analysis and control of a non-local PDE traffic flow model. *International Journal of Control*, **0**(0), 1–19.

Lopez, Pablo Alvarez, Behrisch, Michael, Bieker-Walz, Laura, Erdmann, Jakob, Flötteröd, Yun-Pang, Hilbrich, Robert, Lücken, Leonhard, Rummel, Johannes, Wagner, Peter, & Wießner, Evamarie. 2018. Microscopic Traffic Simulation using SUMO. *In: The 21st IEEE Int. Conference on Intelligent Transp. Systems*. IEEE.

Montanaro, Umberto, Dixit, Shilp, Fallah, Saber, Dianati, Mehrdad, Stevens, Alan, Oxtoby, David, & Mouzakitis, Alexandros. 2019. Towards connected autonomous driving: review of use-cases. *Vehicle System Dynamics*, **57**(6), 779–814.

Papageorgiou, M, Marinaki, M, Typaldos, P, & Makantasis, K. 2016. A feasible direction algorithm for the numerical solution of optimal control problems–extended version. *Chania, Greece: Technical University of Crete, Dynamics Sysyems and Simulations Laboratory*, 2016–26.

Papageorgiou, M., Mountakis, K. S., Karafyllis, I., Papamichail, I., & Wang, Y. 2021. Lane-Free Artificial-Fluid Concept for Vehicular Traffic. *Proceedings of the IEEE*, **109**(2), 114–121.

Troullinos, D., Chalkiadakis, G., Papamichail, I., & Papageorgiou, M. 2021. Lane-Free Microscopic Simulation for Connected and Automated Vehicles. *In: 2021 24th IEEE Int. Conference on Intelligent Transp.*